

# **Asymmetric Fission across the Nuclear Chart**

Takatoshi Ichikawa, Yukawa Institute, Kyoto

Peter Moller, PMSCG, Los Alamos

- COLLABORATORS ON OTHER PROJECTS  
TOO NUMEROUS TO LIST
- SO PLEASE CONSULT MY WEB PAGE FOR NAMES  
AND ASSOCIATED PROJECTS:
- **<https://t2.lanl.gov/nis/molleretal/>**

# MAIN POINTS

- Possibility of asym. in R.E. proposed 50+ years ago based on highly model-independent arguments
- Does saddle asym? mean fragment asym.?
- How know you have found the “mechanism”
- Benchmark models wrt known data first(!)  
and show useful agreement
- Can (and should) you explain everything “simply”
- “Scientific Method”



# The microscopic mechanism behind the fission-barrier asymmetry (II): The rare-earth region $50 < Z < 82$ and $82 < N < 126$

T. Ichikawa<sup>a</sup>, P. Möller<sup>b,c,\*</sup>

<sup>a</sup> Yukawa Institute for Theoretical Physics, Kyoto University, Kyoto 606-8502, Japan

<sup>b</sup> Theoretical Division, Los Alamos National Laboratory, Los Alamos, NM 87544, USA

<sup>c</sup> P. Moller Scientific Computing and Graphics, Inc., P. O. Box 1440, Los Alamos, NM 87544, USA

## ARTICLE INFO

### Article history:

Received 5 September 2018

Received in revised form 4 December 2018

Accepted 14 December 2018

Available online 19 December 2018

Editor: W. Haxton

### Keywords:

Fission

Fission-fragment mass asymmetry

Single-particle levels

## ABSTRACT

It is well known that most actinides fission into fragments of unequal size. This contradicts liquid-drop-model theory from which symmetric fission is expected. The first attempt to understand this difference suggested that division leading to one of the fragments being near doubly magic  $^{132}\text{Sn}$  is favored by gain in binding energy. After the Strutinsky shell-correction method was developed an alternative idea that gained popularity was that the fission saddle might be lower for mass-asymmetric shapes and that this asymmetry was preserved until scission. Recently it was observed [Phys. Rev. Lett. 105 (2010) 252502] that  $^{180}\text{Hg}$  preferentially fissions asymmetrically in contradiction to the fragment-magic-shell expectation which suggested symmetric division peaked around  $^{90}\text{Zr}$ , with its magic neutron number  $N = 50$ , so it was presented as a “new type of asymmetric fission”. However, in a paper [Phys. Lett. B 34 (1971) 349] a “simple” microscopic mechanism behind the asymmetry of the actinide fission saddle points was proposed to be related to the coupling between levels of type  $[40\Lambda\Omega]$  and  $[51\Lambda\Omega]$ . The paper then generalizes this idea and made the remarkable prediction that analogous features could exist in other regions. In particular it was proposed that in the rare-earth region couplings between levels of type  $[30\Lambda\Omega]$  and  $[41\Lambda\Omega]$  would favor mass-asymmetric outer saddle shapes. In this picture the asymmetry of  $^{180}\text{Hg}$  is not a “new type of asymmetric fission” but of analogous origin as the asymmetry of actinide fission. This prediction has never been cited in the discussion of the recently observed fission asymmetries in the “new region of asymmetry”, in nuclear physics also referred to as the rare-earth region. We show by detailed analysis that the mechanism of the saddle asymmetry in the sub-Pb region is indeed the one predicted half a century ago.

© 2018 The Authors. Published by Elsevier B.V. This is an open access article under the CC BY license (<http://creativecommons.org/licenses/by/4.0/>). Funded by SCOAP<sup>3</sup>.

## 1. Introduction

The discovery of fission in 1938 was based on the identification of barium ( $Z = 55$ ) in the products following bombardment of uranium with neutrons [1]. An immediate intuitive theoretical model providing a picture of the phenomenon in terms of the deformation of a charged liquid drop with a surface tension was given by Meitner and Frisch [2]. The discovery and its interpretation was further confirmed by observation of the high kinetic energies of the fission fragments [3]. About half a year later Bohr and Wheeler provided a more complete theoretical and quantitative discussion of the observed fission process by generalizing the semiempirical

mass model [4] into a liquid-drop model of the nuclear potential energy as a function shape [5].

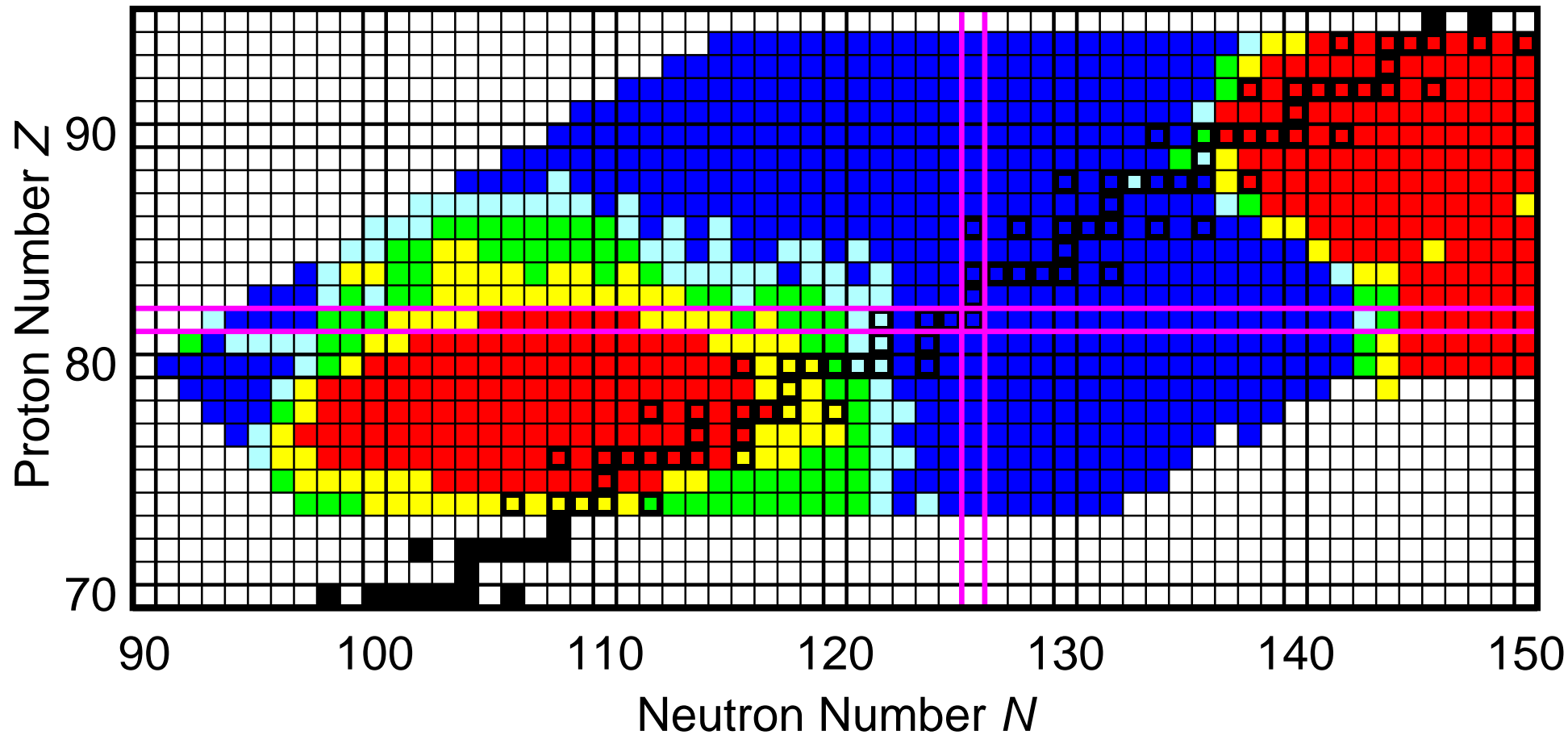
However, the liquid-drop model theory did not explain the observations that the preferred mass split, of the light actinide systems studied at the time, was asymmetric mass division with a heavy fragment with nucleon number  $A \approx 140$  and the remaining nucleons in a smaller fragment. The energetically preferred division in liquid-drop model theory is symmetric. Since the discovery of fission a subject of intense interest has been and still is to explain the observed fission asymmetry and ideally to model more exactly the observed yield distributions.

An initial qualitative theoretical interpretation for the experimental observations of asymmetric fission was that fissioning systems favor division into a heavy fragment near the doubly magic  $^{132}\text{Sn}$  because the magic proton number  $Z = 50$  and neutron number  $N = 82$  and associated microscopic effects result in an extra binding of about 12 MeV in  $^{132}\text{Sn}$  relative to liquid-drop theory. In

\* Corresponding author at: P. Moller Scientific Computing and Graphics, Inc., P. O. Box 1440, Los Alamos, NM 87544, USA.

E-mail address: [mollerinla@gmail.com](mailto:mollerinla@gmail.com) (P. Möller).

# Fission-Fragment Symmetric-Yield to Peak-Yield Ratio



# THE MICROSCOPIC MECHANISM BEHIND THE FISSION BARRIER ASYMMETRY

C. GUSTAFSSON, P. MÖLLER and S. G. NILSSON

*Lund Institute of Technology, Lund, Sweden*

Received 14 January 1971

The instability at the second saddle point of actinide elements towards asymmetric distortions is explained by a decrease in energy of the neutron orbitals  $[40\Lambda\Omega]$  (orbitals at the waistline of the nucleus) for asymmetric distortions. These orbitals are situated at the Fermi surface and couple strongly to  $[51\Lambda\Omega]$  levels slightly above the Fermi surface.

In a recent publication [1] we exhibited the results of calculations (based on the Strutinsky shell correction method [2]) that in addition to  $P_2$  and  $P_4$  distortions also included the asymmetric  $P_3$  and  $P_5$  degrees of freedom. In the region  $N = 130$ -150 we encountered for  $\epsilon = 0.85$  a tendency to asymmetric distortions. The second barrier peak was found to be reduced by 2 - 2.5 MeV for  $^{236}\text{U}$  due to the combined effect of  $P_3$  and  $P_5$  distortion. On the other hand for  $^{248}\text{Cf}$  the combined effect in reducing the barrier was less than 0.5 MeV. Finally  $^{210}\text{Po}$  was found to be stable at all  $\epsilon$ -values between 0.0 and 1.0. Recent communications from Pauli et al. [3] indicate very similar results on  $P_3 + P_5$  instability reached on the basis of their radially somewhat different potential.

Asymmetry favouring orbitals. Since the early calculations involving only a few representative nuclei, also intermediary nuclei were studied by one of us [4] and the collected results on the possible  $P_3$  and  $P_5$  instability for the point  $\epsilon = 0.85$ ,  $\epsilon_4 = 0.12$ , which represents the approximate locus of the second barrier peak for actinide nuclei, are found in fig. 1. This figure thus exhibits the transition lines in  $A$  and  $Z$  for nuclei where the asymmetric degrees of freedom start to affect the height of the second barrier.

Although the tendency to asymmetry was clearly established as a single-particle effect in ref. [1], no detailed "microscopic" explanation was given in terms of specific orbitals. (From the rapid variation in the mass distribution of the fission fragments from  $^{210}\text{Po}$  to  $^{236}\text{U}$  to  $^{252}\text{Fm}$  it is obvious that a shell structure explanation is called for and that this rapid variation

hardly can be explained in terms of the smooth variations with  $Z$  and  $A$  of the liquid-drop model.)

In the calculations of ref. [1] we assumed a potential of the following type [5,6]

$$V = \frac{1}{2} \hbar \omega_0 (\epsilon, \epsilon_4, \epsilon_1, \epsilon_3, \epsilon_5) \rho^2 \times$$

$$[1 - \frac{2}{3} \epsilon P_2 + 2\epsilon_4 P_4 + 2\epsilon_1 P_1 + 2\epsilon_3 P_3 + 2\epsilon_5 P_5] - V_{\text{corr}}$$

$$V_{\text{corr}} = \kappa \hbar \omega_0 (2I_t \cdot s + \mu(I_t^1 - \langle I_t^1 \rangle_{\text{shell}}))$$

where the amount of  $P_1$  distortion is determined so as to compensate the center-of mass displacement involved in the addition of  $P_3$  and  $P_5$

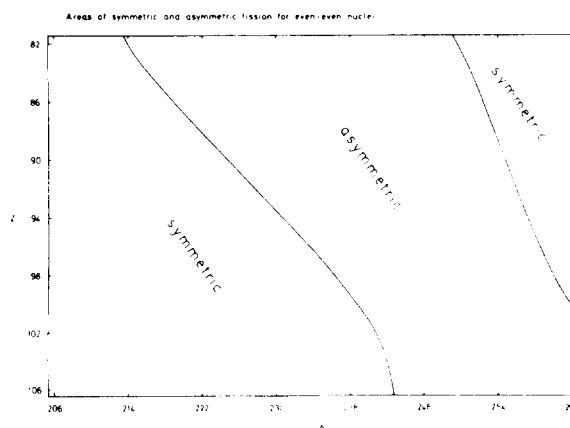


Fig. 1. Map of energy stability at the second barrier peak ( $\epsilon = 0.85$ ,  $\epsilon_4 = 0.12$ ) according to calculations in terms of the asymmetry parameter  $\epsilon_3(\epsilon_5)$  for an area of  $Z$ - and  $N$ -values. It is found that the region of instability of actinide elements involves a limited number of  $N$ -values generally up to  $N \approx 160$ , and starting at  $N \approx 132$ .

terms. In this paper, a simple calculation of the following kind has been performed. Starting from the position  $\epsilon = 0.85$ ,  $\epsilon_4 = 0.12$ , which, as mentioned, roughly corresponds to the second

saddle point in the  $(\epsilon, \epsilon_4)$  plane, we have plotted the single-particle energy levels as functions of  $\epsilon_3(\epsilon_5)$ . (The notation  $\epsilon_3(\epsilon_5)$  implies that for each  $\epsilon_3$  we employ the  $\epsilon_5$ -value that gives minimum

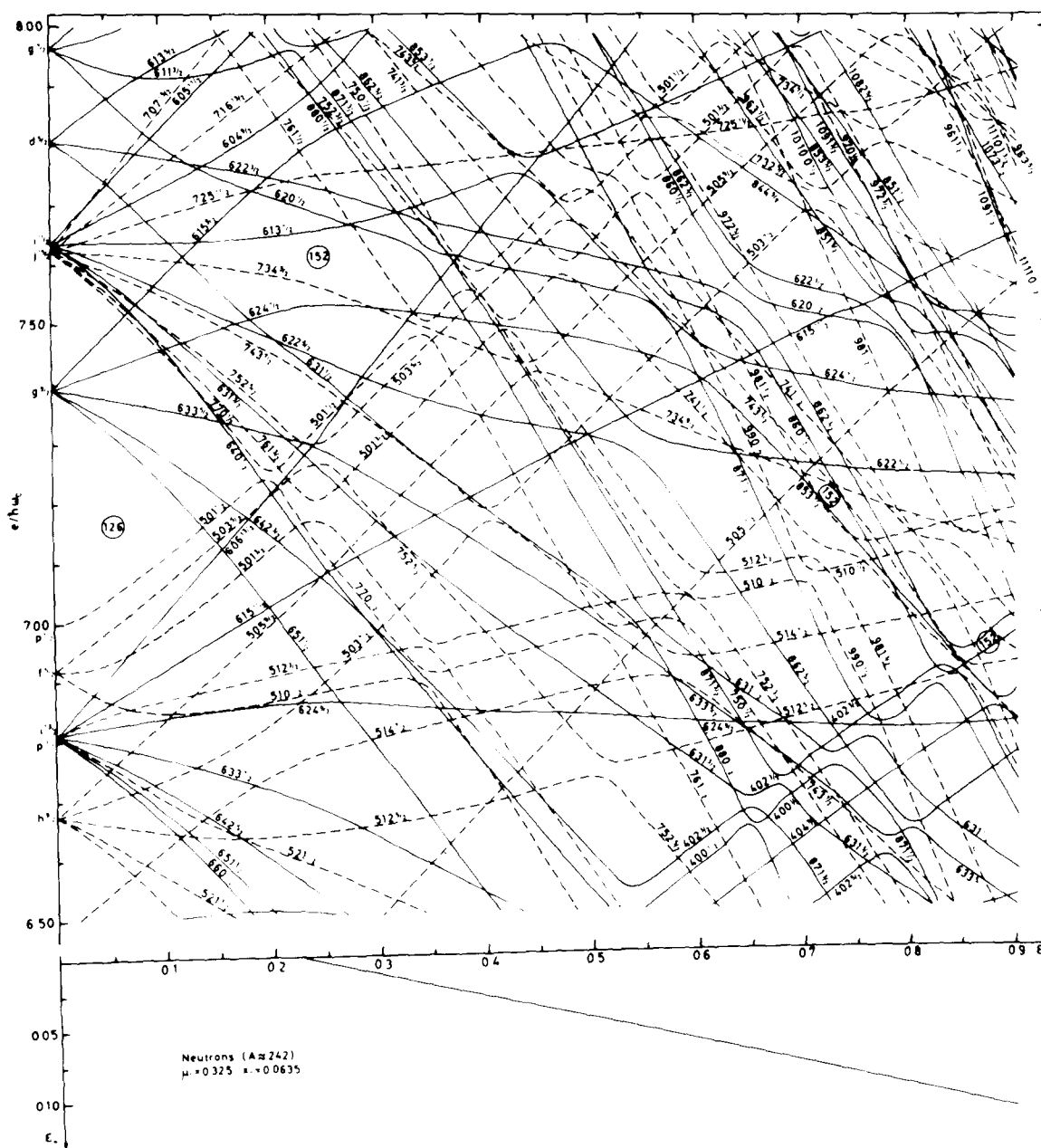


Fig. 2. Single-neutron orbitals in the actinide region as a function of  $\epsilon$ . To each  $\epsilon$ -value corresponds a value of  $\epsilon_4$  as marked below in the figure. This relation roughly coincides with the assumed "fission path" in the  $(\epsilon, \epsilon_4)$  plane. Note in the lower right corner of the figure the emergence of the  $[40 \times]$  levels, which are found to be largely responsible for the asymmetry, and above them the  $[51 \times]$  levels strongly coupled to the former by the octupole term in the potential.

total energy.) The entering neutron orbitals are first identified in fig. 2 [7] which shows the single-particle levels as functions of  $\epsilon_2(\epsilon_4)$ . (The  $\epsilon_4$ -values in the corresponding calculation are

chosen as indicated below in the figure and so as to reproduce the "path" to fission in the  $(\epsilon, \epsilon_4)$ -plane.) Although many quasi-crossings, with orbitals approaching each other closely, occur for

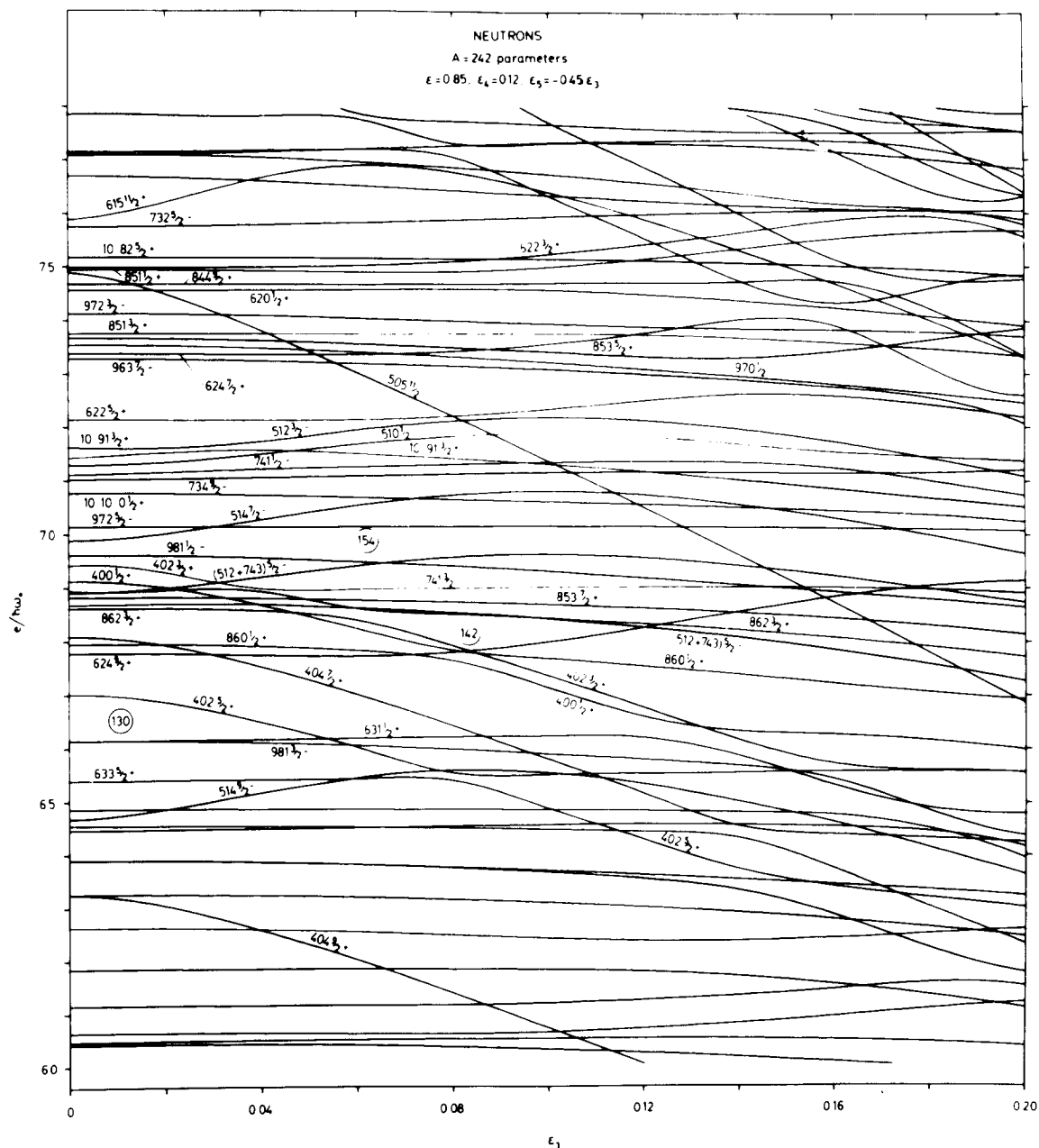


Fig. 3. Single-neutron levels for  $\epsilon = 0.85$ ,  $\epsilon_4 = 0.12$  as functions of the asymmetric distortion coordinate  $\epsilon_3(\epsilon_5)$ . Note the strong downward curvature of the  $[40 \times]$  levels as well as of the orbital  $[505 11/2]$  and the upward curvature of the  $[51 \times]$  levels, which for  $N=150$  are as yet unfilled for the large  $\epsilon$ -distortions.

## Nilsson's research group

Sven Gösta built up an enthusiastic research group, and Lund became an important centre for theoretical nuclear structure research. He created a familiar and creative atmosphere, and showed great interest not only in his PhD students, but also their families.

Nuclear physicists from around the world were anxious to discuss research with him. Lund continued to be an internationally leading centre for research into theoretical nuclear models after his untimely death in 1972.



Sven Gösta Nilsson together with members of his research group at the beginning of the 1970s.

Standing from the left:

Gunnar Ohlén, Christer Gustafsson, Ingemar Ragnarsson, Stig Erik Larsson, Reginald Boleu, Johan Claesson, and Petr J aneček.

Sitting:

Sven Bertil Nilsson, Peter Möller, Zdzisław Szymáński, Sven Gösta Nilsson, and Thomas Johansson.



# S.A.E. Johansson 1961 RE asym suggestion

In 1961 Sven Johansson suggested that couplings between levels of opposite parity could lead to asymmetric fission where these specific situations in single-particle level structure occurred. In the last line of the paper he proposed this could occur in the rare-earths.

## NUCLEAR OCTUPOLE DEFORMATION AND THE MECHANISM OF FISSION

SVEN A. E. JOHANSSON

*Department of Physics, University of Lund, Lund, Sweden*

Received 20 October 1960

**Abstract:** The stability of nuclei against an octupole deformation has been calculated. It is found that the interaction of levels of opposite parity makes the nuclei in certain regions very soft to octupole deformation. The negative parity collective states in heavy nuclei and in the rare earth region can be interpreted as octupole vibrations. The predicted  $A$ -dependence of the energy of these states agrees well with experimental data.

For very elongated shapes, which are of interest in fission, it is found that stable octupole deformation occurs. The potential surface of the fission barrier will therefore possess two asymmetric valleys. There is a linear relationship between the mass ratio of the fission fragments and the degree of octupole deformation at the saddle point. The occurrence of symmetric fission in the lighter elements is explained. The influence of the octupole deformation on the fission barrier also provides a basis for understanding the variation in fission threshold. The experimental data agree with the calculated values. The peak to valley ratio in the mass distribution is calculated, with the assumption of statistical equilibrium at the saddle point. Good agreement is found for excitation energies below 10 MeV. For higher energies a symmetric component appears which rises with increasing energy.

### 1. Introduction

Nuclear deformation of the octupole type is of interest in several ways. It was suggested by Christy <sup>1)</sup> that the low-energy negative parity states in heavy nuclei could be explained as octupole vibrations. Strutinsky <sup>2)</sup> pointed out that the coupling between a filled and an unfilled level of opposite parity gives a tendency towards octupole deformation. This problem was investigated more in detail by Lee and Inglis <sup>3)</sup>. Using perturbation theory and assuming a spheroidal harmonic-oscillator potential, they calculated the strength of the deforming force. They concluded that the decrease in energy due to this effect is not quite enough to overcome the increase arising from the requirement of volume conservation. Because of the simple potential used the right level order is not reproduced and it is not possible to compare the results of this calculation with the situation in any real nuclei. Furthermore, the neglect of the spin-orbit coupling will have a decisive influence on the calculations. The spin-orbit coupling will bring the interacting levels closer together and hence increase the deforming force.

give only a small contribution to  $E_1$ . The volume conservation energy  $E_2$ , which opposes the tendency to pear-shape, does not depend so strongly on the character of the levels and hence increases rather regularly as the mass number increases. The result will thus be that above thorium the nuclei will become less soft to the octupole deformation and the energy of the 1— state will increase. In the rare earth region we expect a similar situation, since these nucleides have a configuration which is rather similar to that of the heavy ones.

When the elongation of the nucleus is increased, (18) makes possible a crude estimate of the equilibrium octupole deformation. The deformation energy parameter  $C$  and the matrix elements  $M_{ab}$  do not vary much with the deformation and for the present purpose they can be considered as constant.  $C$  can easily be estimated as well as  $n$ , the number of matrix elements which are great enough to give an appreciable contribution to the deforming force. The distance between the interacting levels  $\Delta E$  is given by (11). At the equilibrium elongation we can set  $\alpha'_3 = 0$  since the nucleus is here very soft to octupole deformation and this implies  $C = n\bar{M}_{ab}/\Delta E_{eq}$ , where  $\Delta E_{eq}$  is the level distance at the equilibrium elongation. Hence we get directly  $\bar{M}_{ab}$ . If this value is inserted in (18) we get the following approximate expression:

$$\alpha'_3 = \left(\frac{n}{2C}\right)^{\frac{1}{2}} \left(\frac{\Delta E_{eq}^2 - \Delta E^2}{\Delta E_{eq}}\right)^{\frac{1}{2}}. \quad (24)$$

We see immediately that  $\alpha'_3$  increases when the elongation is increased, since  $\Delta E$  decreases. It will be noted that  $\alpha'_3$  does not depend strongly on  $C$  or  $n$ . The values calculated according to (24) agree reasonably well with the result of the more exact calculation.

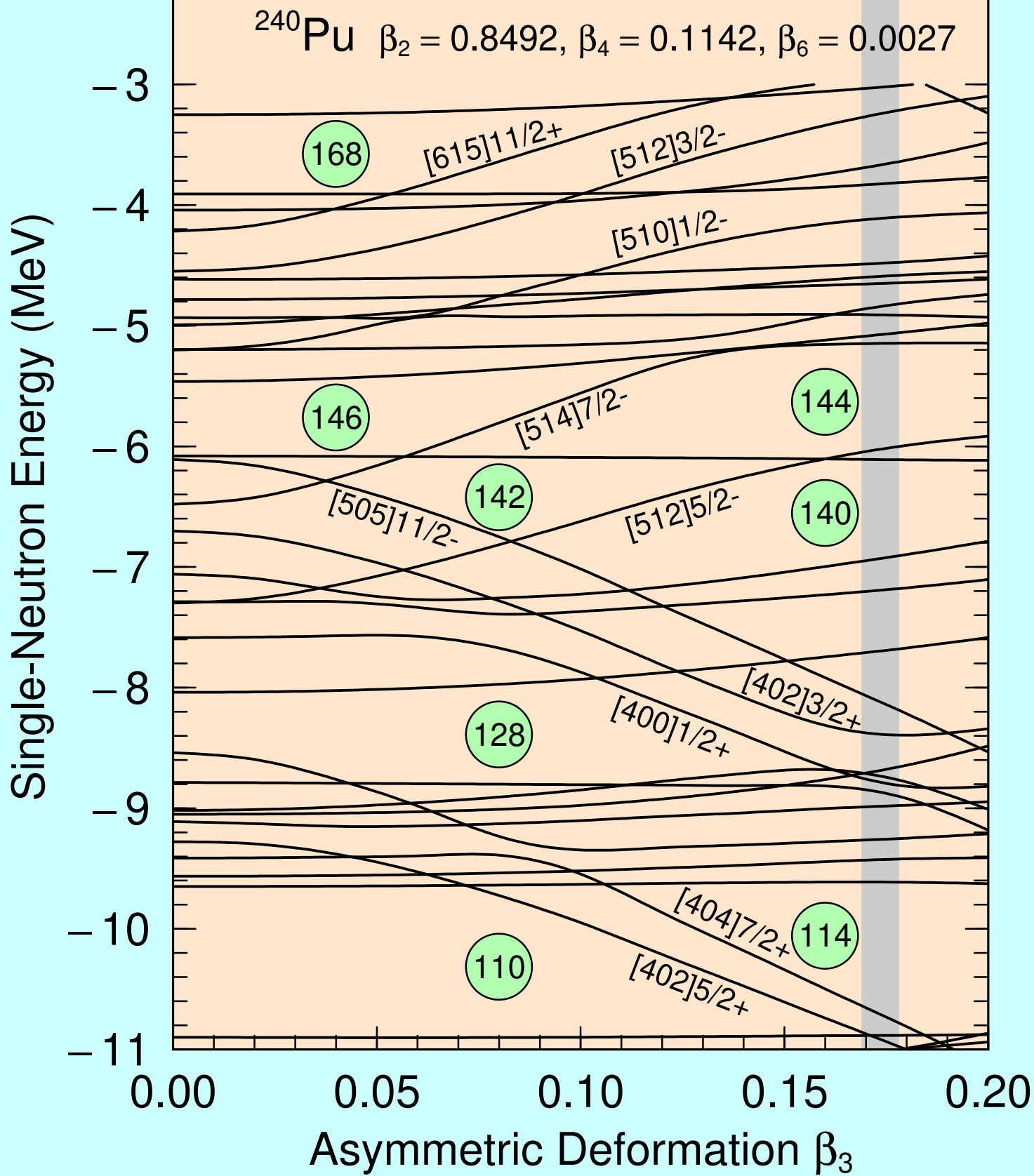
As was discussed above  $n$  will decrease for large deformations due to the transfer of nucleons to other levels. As can be seen from (18),  $\alpha'_3$  will decrease and eventually become imaginary, corresponding to a symmetric saddle point. Also in this case a crude estimate shows good agreement with the detailed calculation.

This discussion shows that the main results can be derived from the general properties of the level diagram and the matrix elements. They are not critical in regard to the details of the level diagram or the assumed nuclear configuration.

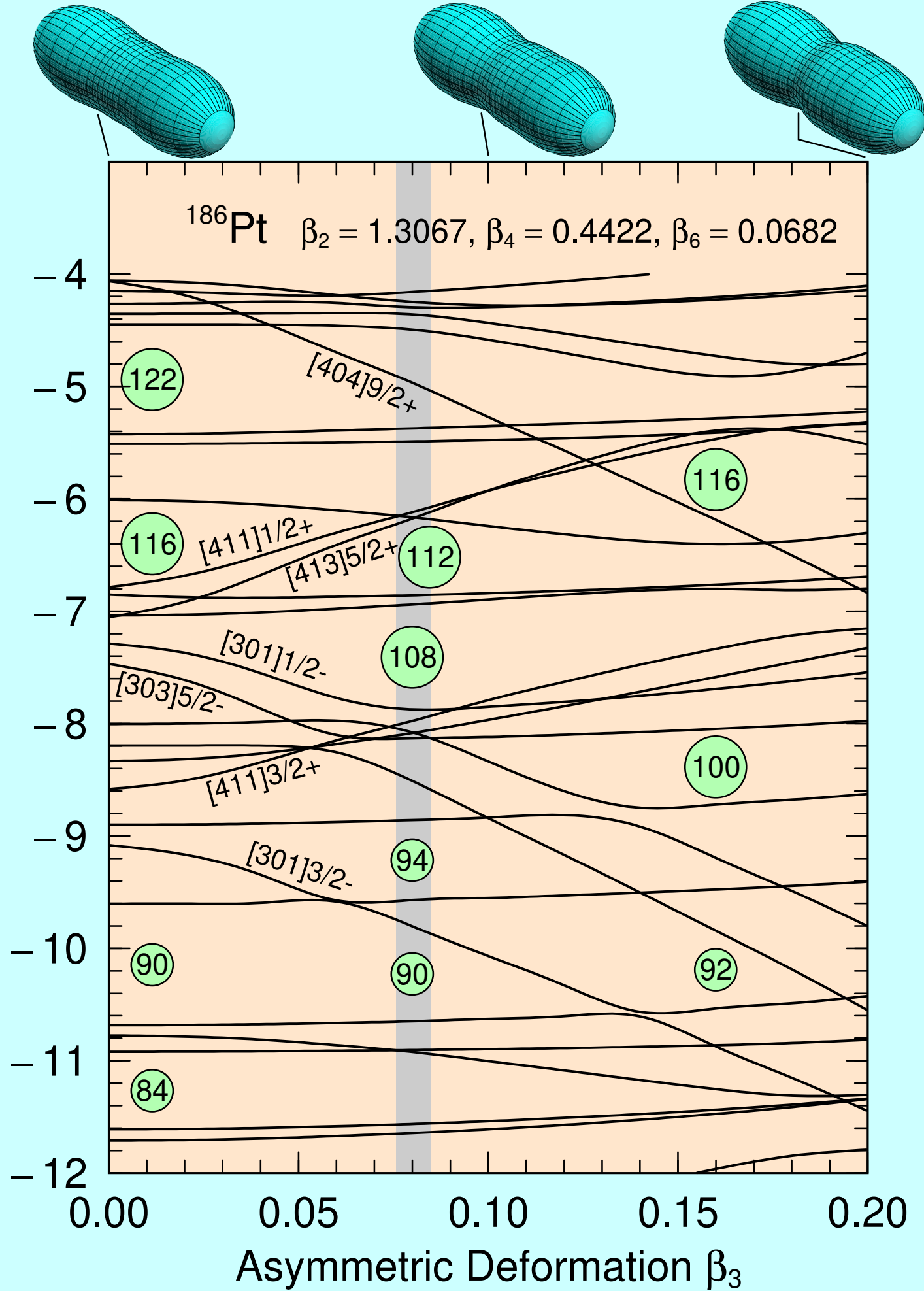
The present calculations are necessarily simplified in several respects, but still they seem to be able to reproduce the experimental facts quite well. When more experimental data become available an even better comparison between theory and experiment can be made. Several interesting experiments are suggested by these calculations. It would, for example, be of great value to know more about the various fission parameters in the transition region around radium. A systematic study of fission in the rare earth region would also be of interest.

The author would like to thank Professor T. Gustafson, Professor B. R. Mottelson and Dr. S. G. Nilsson for helpful discussions.

In PLB 34B(1971)349 it was shown that mass-asymmetric shapes led to splitting of levels of opposite parity at light actinide saddle points and consequently to mass-asymmetric saddle points. It was proposed that the same mechanism would occur at one lower main oscillator quantum number  $N$  at rare-earth saddle points. The next two slides show this prediction is correct.



Single-Neutron Energy (MeV)



At this time a strong correlation was observed between calculated degree of asymmetry at the saddle point and observed fragment mass asymmetries, see figure in the following paper.

On the page following the figure it is pointed out that a displayed 2D potential-energy surface, which is a function of additional variables that cannot be visualized in 2D plots must be continuous in the additional variables.

Discontinuities in HFB calculations with respect to unconstrained variables are a common occurrence. The “lines of discontinuity” that occur in 2D HFB potential-energy surfaces are not at all related to scission configurations but to vastly inadequate and discontinuous deformations. This is recognized by some in the HFB community, see for example Dubray and Regnier *Comp. Phys. Comm.* **183** (2012) 2035.



## ODD-MULTIPOLE SHAPE DISTORTIONS AND THE FISSION BARRIERS OF ELEMENTS IN THE REGION $84 \leq Z \leq 120$

P. MÖLLER

*Department of Mathematical Physics, University of Lund, Technical Faculty, Lund, Sweden*

Received 12 November 1971

(Revised 24 February 1972)

**Abstract:** Potential-energy surfaces have been studied for a large number of nuclei in the region  $84 \leq Z \leq 120$ . The shapes of the studied nuclei correspond to a continuous sequence from a spherical shape to distortions slightly beyond the outer saddle taking into account both symmetric and asymmetric deformations. The effect of asymmetric distortions is studied in detail. It is found that the second saddle of the actinide elements is asymmetrically distorted. The size of the asymmetry is a sensitive function of the neutron number and generally of the position of specific orbitals in the single-particle energy level diagrams. The amount of asymmetric distortions at the outer saddle is also well correlated to the experimental mass ratios in low-energy or spontaneous fission. From the calculated potential-energy surfaces fission-barrier parameters are determined for some 50 nuclei in the region.

Results pertinent to the superheavy region indicate that the barrier heights are not reduced by taking asymmetric distortions into account in the calculations. From the potential-energy surfaces obtained it seems probable that the mass distribution of the fission products is symmetric for superheavy elements near  $Z = 114$ ,  $N = 184$ .

### 1. Introduction

A great break-through in the investigation of the fission process and in particular, the fission barrier was initiated by the experimental discovery of fission shape isomeric states by Polikanov <sup>1)</sup> and Flerov <sup>2)</sup>. This greatly stimulated the development of a new and realistic method of calculating the nuclear potential-energy surface. This new approach results from regarding the nuclear potential energy as a sum of one macroscopic and one microscopic contribution. The macroscopic part is assumed to be described by the liquid-drop model. This model reproduces on the average the nuclear potential energy as a smooth function of distortion, mass number ( $A$ ) and charge number ( $Z$ ). In particular it accounts well for the gross variations of the nuclear ground state masses with  $Z$  and  $A$ . However, superimposed on the smooth average behaviour of the nuclear masses described by the liquid-drop theory there are fluctuations that are rapidly varying functions of distortion, mass and charge number. These fluctuations are caused by single-particle effects and constitute the microscopic part of the nuclear potential energy.

Early calculations in this spirit, attempting to take shell effects into account in the treatment of fission were those undertaken by Swiatecki <sup>3)</sup> and by Johansson <sup>4, 5)</sup>.

For spontaneously fissioning nuclei one finds experimentally on the average a

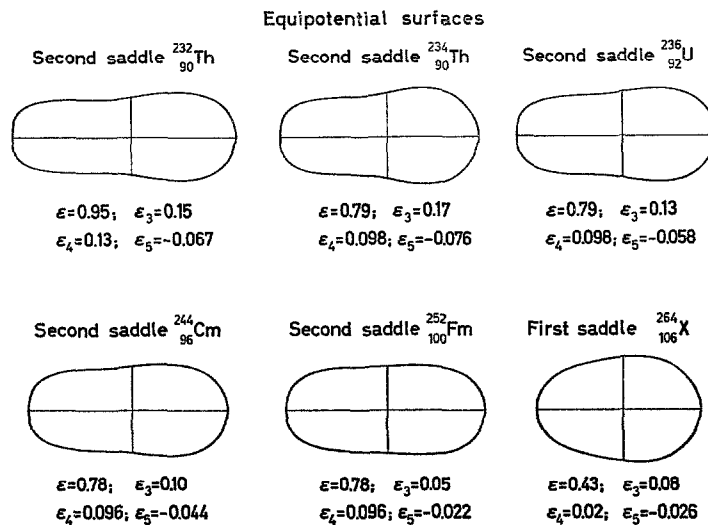


Fig. 16. Equipotential shapes at saddle point distortions for a number of nuclei in the region  $84 \leq Z \leq 106$ , calculated with  $(G \cup S, \kappa_s = 1.78)$ . The shapes obtained are obviously rather smooth.

of the nucleus the mass distribution is decided. One point of view is that the mass distribution is decided already at saddle point distortions, i.e. where the nucleus is cold. For the heavier actinides beyond Pu the second saddle is lower than the first. Nevertheless as it lies not far below and is still above the ground state it is probable that conditions at the second saddle also in these cases will influence the mass distribu-

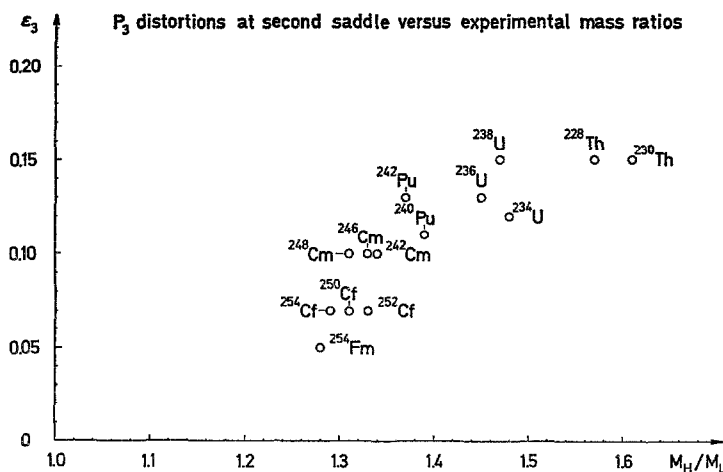


Fig. 17.  $P_3$  distortions of the second saddle calculated with  $(G \cup S, \chi_s = 1.78)$ , versus the experimental mass ratios of the fission fragments.  $M_H$  is the mass of the heavy fragment and  $M_L$  the mass of the light fragment. There appears to be a fairly good correlation, a result also obtained by Johansson <sup>5)</sup> and Pauli *et al.* <sup>27)</sup>.

0.70, ... 1.00) and 7 equidistant values of  $\varepsilon_3$  ( $\varepsilon_3 = 0.00, 0.04, \dots, 0.24$ ). A number of the potential-energy surfaces obtained are displayed in figs. 14a–z. Most of the contour maps shown are for ( $G \sim S, \kappa_s = 1.78$ ) but some results with the alternative choice of pairing and surface symmetry parameters ( $G = \text{const.}, \kappa_s = 2.53$ ) are

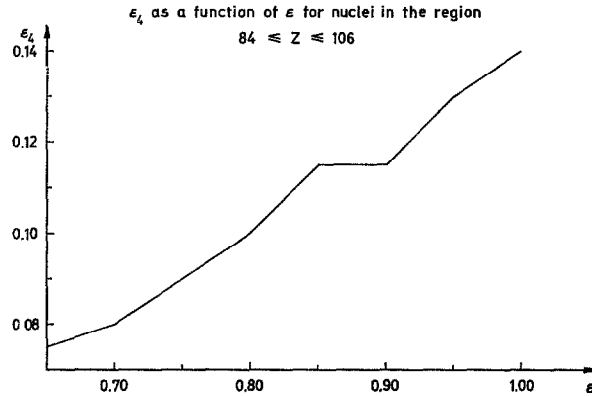
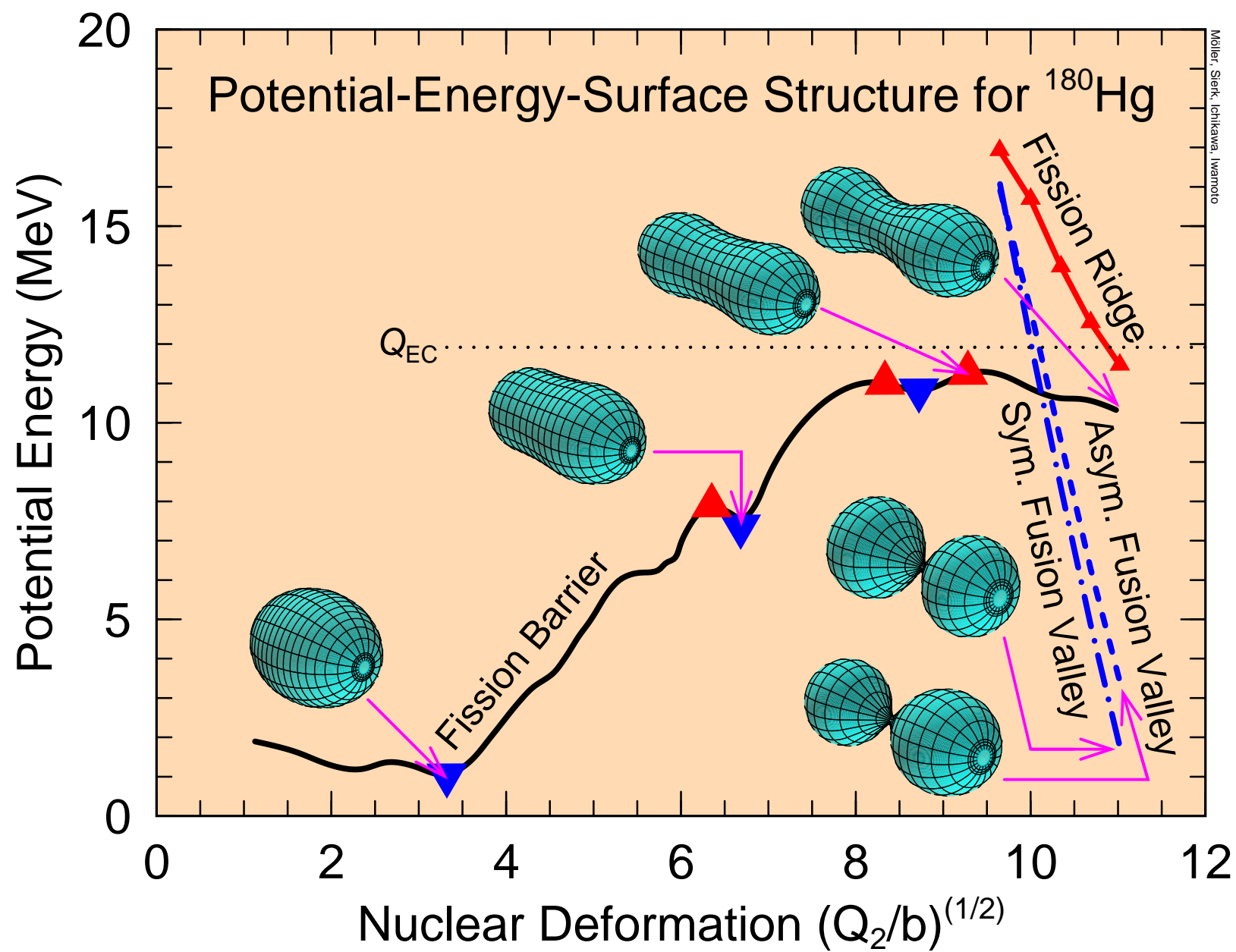


Fig. 13. Definition of the dependent variable  $\varepsilon_4$  as a function of  $\varepsilon$ , as employed in the calculations of the potential-energy surfaces exhibited in figs. 14a–z.

displayed for comparison. We see that for most nuclei in these plots there is an instability of the second saddle point to asymmetric distortions. Approximately we have stability for  $N < 132$ , (e.g.  $^{210}_{84}\text{Po}$ ,  $^{220}_{88}\text{Ra}$ ) while for  $N > 132$  we have an instability that increases with neutron number until the neutron number reaches about 146 after which there is a decrease of the instability. This is in agreement with the approximate conclusions that can be drawn from the shell-correction diagrams in figs. 5a and b. We note that the asymmetric saddle has an  $\varepsilon$ -value that is usually different from that of the symmetric saddle. This is why we cannot draw any definite conclusion on the magnitude of the asymmetry effect at the second saddle from the shell-correction diagrams in figs. 5a and b as  $\varepsilon$  in these figures is kept at the fixed value 0.85.

We note that although the contour maps in figs. 14a–z are displayed as functions of two parameters only, this does not mean that in the determination of the outer saddle we have limited ourselves to a two-dimensional approximation of the multi-dimensional problem. As stated above the value of the dependent parameter  $\varepsilon_5$  is in each point such that the energy is minimized with respect to  $\varepsilon_5$ . Thus figs. 14a–z are projections of surfaces through the saddle points in three-dimensional ( $P_2 + P_4, P_3, P_5$ ) space to the two-dimensional space ( $P_2 + P_4, P_3 + P_5$ ), and the energy values of the saddle points in figs. 14a–z are the same as in three-dimensional ( $P_2 + P_4, P_3 - P_5$ ) space. It is important to note that the value of  $\varepsilon_5$  corresponding to the points  $\varepsilon, \varepsilon_3$  in figs. 14a–z is a continuous function of  $\varepsilon$  and  $\varepsilon_3$ . This means that we have not inadvertently tunneled through a mountain ridge separating two valleys in ( $P_2 + P_4, P_3, P_5$ ) space, in which case our value for the saddle point might have been too low.

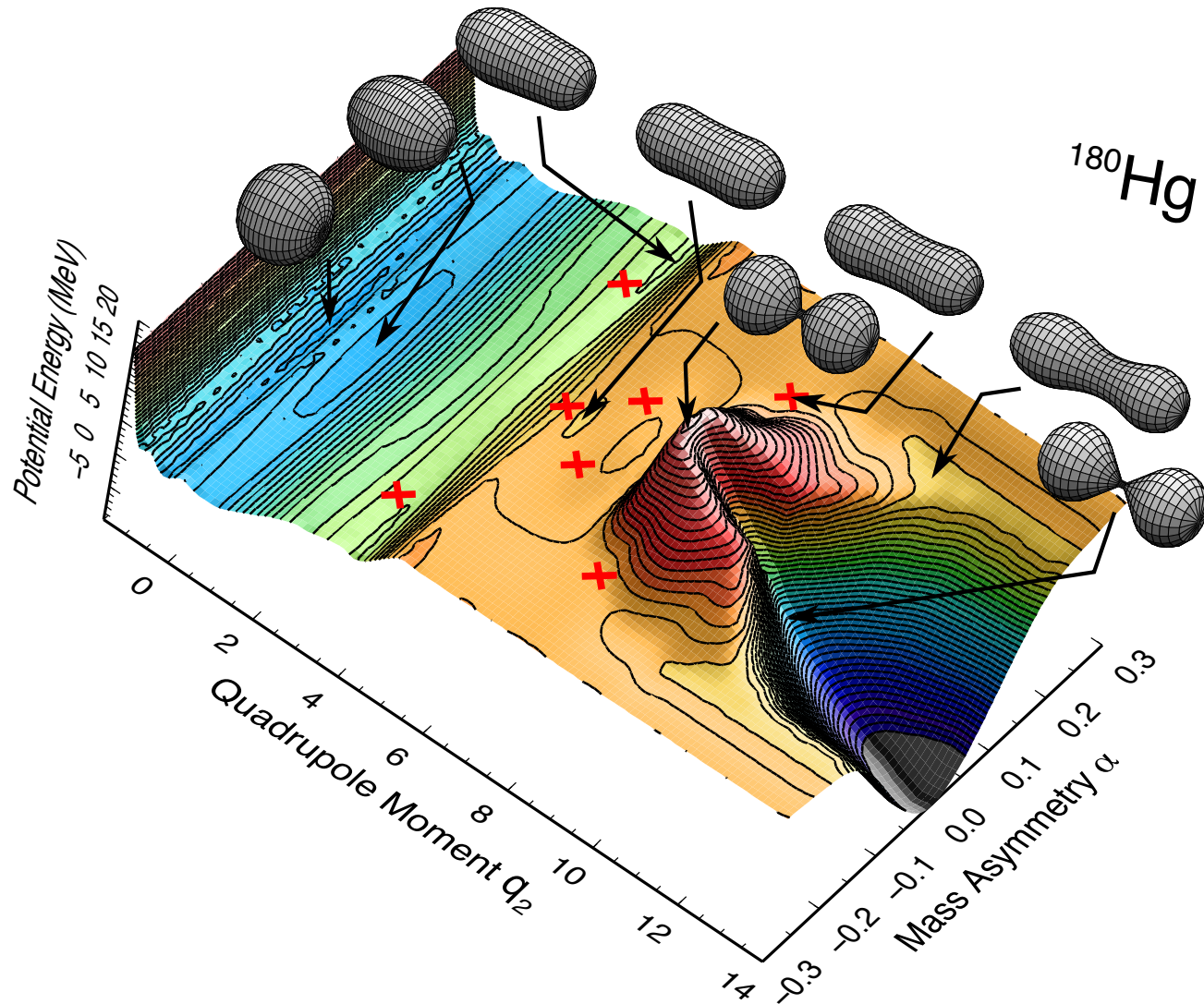


$^{180}\text{Hg}$

Potential Energy (MeV)  
-5 0 5 10 15 20

Quadrupole Moment  $q_2$   
0 2 4 6 8 10 12 14

Mass Asymmetry  $\alpha$   
-0.3 -0.2 -0.1 0.0 0.1 0.2 0.3



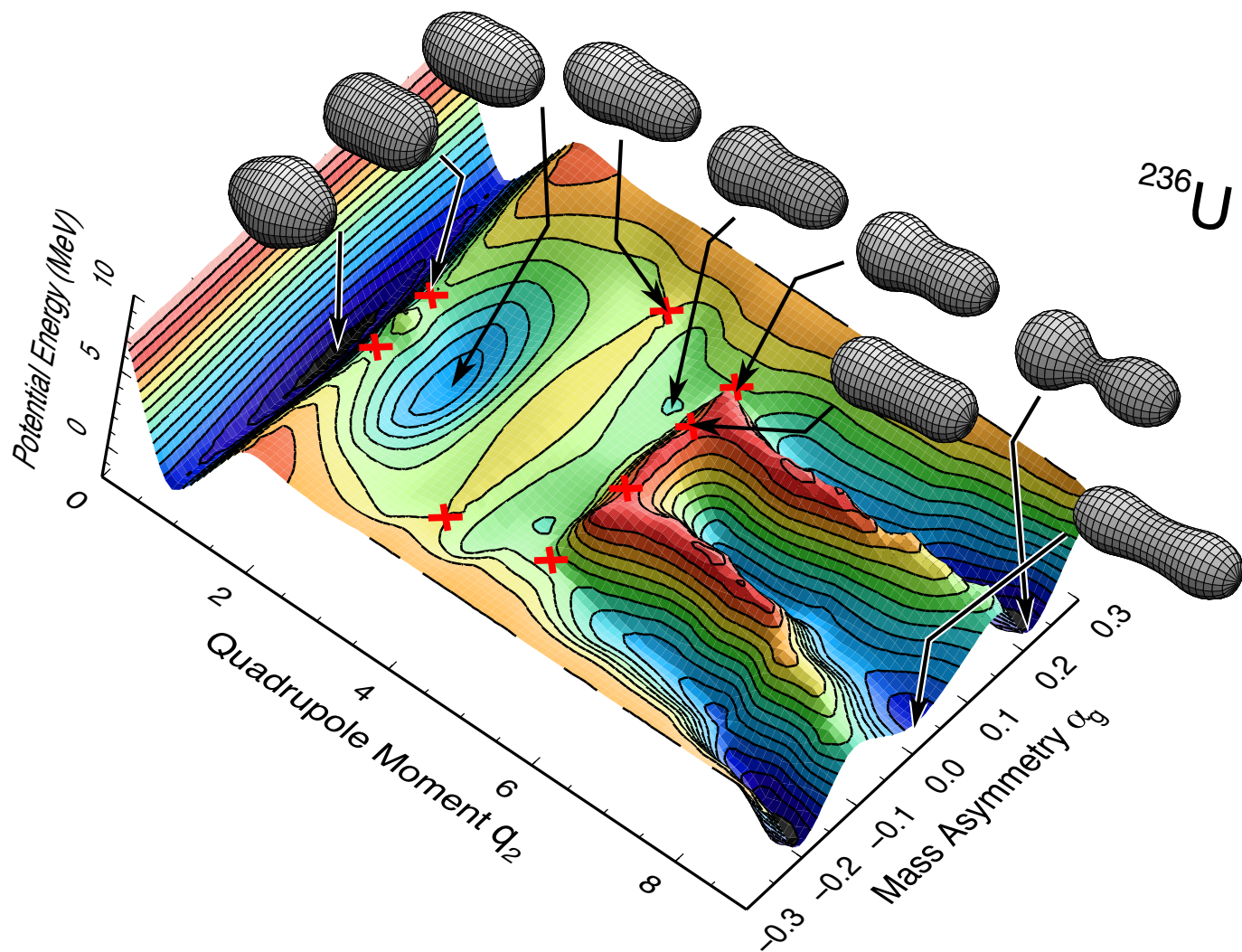


Table 1: Saddle shell corrections

<b>Nucleus</b>	<b>Symm Saddle</b>	<b>Asym Saddle</b>
$^{236}\text{U}$	3.41	−5.13
$^{178}\text{Pt}$	2.08	−0.68

Already in 1936 in their discussion of the semi-empirical mass model Bethe and Bacher considered that this mass model might be less accurate near “shells” in single-particle models.



# Nuclear Physics

## A. Stationary States of Nuclei<sup>1</sup>

H. A. BETHE AND R. F. BACHER, *Cornell University*

### TABLE OF CONTENTS

#### I. Fundamental Properties of Nuclei

§ 1. CHARGE, WEIGHT.....	83
§ 2. ENERGY.....	85
§ 3. SIZE.....	88
§ 4. STATISTICS.....	89
§ 5. SPIN AND MAGNETIC MOMENT.....	90

#### II. Qualitative Arguments about Nuclear Forces

§ 6. THE RATIO OF ATOMIC WEIGHT TO NUCLEAR CHARGE.....	92
§ 7. SATURATION OF NUCLEAR FORCES.....	93
§ 8. THE ELECTROSTATIC REPULSION OF THE PROTONS. STABILITY AGAINST $\alpha$ -DECAY.....	96
§ 9. DEUTERON AND $\alpha$ -PARTICLE: THE FORM OF THE POTENTIAL FUNCTION.....	99
§ 10. FORCES BETWEEN LIKE PARTICLES. ODD AND EVEN ISOTOPES.....	100

#### III. Theory of the Deuteron

§ 11. THE WAVE EQUATIONS OF HEISENBERG, WIGNER AND MAJORANA.....	105
§ 12. GROUND STATE OF THE DEUTERON.....	108
§ 13. EXCITED STATES OF THE DEUTERON.....	112
§ 14. SCATTERING OF NEUTRONS BY PROTONS. I: CROSS SECTION.....	114
§ 15. SCATTERING OF NEUTRONS BY PROTONS. II: ANGULAR DISTRIBUTION.....	119
§ 16. PHOTOELECTRIC DISINTEGRATION OF THE DEUTERON.....	122
§ 17. CAPTURE OF NEUTRONS BY PROTONS.....	126
§ 18. SCATTERING OF PROTONS BY PROTONS.....	130

#### IV. Theory of $H^3$ , $He^3$ and $He^4$

§ 19. THOMAS' PROOF OF THE FINITE RANGE OF NUCLEAR FORCES.....	134
§ 20. CALCULATION OF THE ENERGY OF $H^3$ , $He^3$ AND $He^4$ FROM THE VARIATION PRINCIPLE.....	137
§ 21. FEENBERG'S "EQUIVALENT TWO-BODY PROBLEM".....	143
§ 22. COMPARISON OF $H^3$ AND $He^3$ .....	146
§ 23. EXCITED STATES OF THE $\alpha$ -PARTICLE.....	147

#### V. Statistical Theory of Nuclei

§ 24. THE HARTREE METHOD.....	149
§ 25. THE STATISTICAL MODEL. QUALITATIVE CONCLUSIONS.....	153

§ 26. QUANTITATIVE RESULTS AND LIMITATIONS OF THE STATISTICAL MODEL.....	157
§ 27. DISPROOF OF ORDINARY FORCES.....	160
§ 28. FORCES BETWEEN LIKE PARTICLES.....	161
§ 29. THE SURFACE EFFECT.....	163
§ 30. WEIZSÄCKER'S SEMIEMPIRICAL FORMULAE.....	165

#### VI. More Detailed Theory of Heavy Nuclei

§ 31. $\alpha$ -PARTICLES AS SUBUNITS OF HEAVIER NUCLEI.....	168
§ 32. QUANTUM STATES OF INDIVIDUAL PARTICLES (NEUTRON AND PROTON "SHELLS").....	171
§ 33. EVIDENCE FOR PERIODICITIES FROM THE ENERGY OF NUCLEI.....	174
§ 34. PERIODICITIES IN THE EXISTING ISOTOPES.....	176
§ 35. ENERGY OF $O^{16}$ AND $Ca^{40}$ IN THE HARTREE APPROXIMATION.....	179
§ 36. THE COUPLING SCHEME IN NUCLEI.....	180
§ 37. VAN VLECK'S POTENTIAL.....	183

#### VII. $\beta$ -Disintegration and Nuclear Forces

§ 38. DISPROOF OF THE EXISTENCE OF ELECTRONS IN NUCLEI.....	184
§ 39. THE NEUTRINO.....	186
§ 40. THEORY OF $\beta$ -DISINTEGRATION.....	189
§ 41. LIFETIME vs. MAXIMUM ENERGY IN $\beta$ -DISINTEGRATION.....	193
§ 42. THE INVERSE $\beta$ -PROCESSES: CAPTURE OF ORBITAL ELECTRONS BY NUCLEI, DISINTEGRATION OF NUCLEI BY ELECTRONS AND NEUTRINOS.....	196
§ 43. STABILITY OF ISOBARS AND FORBIDDEN $\beta$ -PROCESSES.....	198
§ 44. NUCLEAR FORCES AND $\beta$ -DISINTEGRATION.....	201
§ 45. THE MAGNETIC MOMENTS OF PROTON AND NEUTRON.....	205

#### VIII. Nuclear Moments

§ 46. THE INTERACTION OF THE NUCLEAR MOMENT WITH THE ELECTRONS.....	207
§ 47. METHODS USED TO DETERMINE THE NUCLEAR ANGULAR MOMENTUM AND THE HYPERFINE STRUCTURE SEPARATIONS.....	211
§ 48. VALUES OF NUCLEAR SPINS AND MAGNETIC MOMENTS.....	215
§ 49. ISOTOPE SHIFT IN ATOMIC SPECTRA.....	223
§ 50. QUADRUPOLE MOMENTS.....	225

<sup>1</sup> The present issue contains Part A of this report. Part B, treating the dynamics of nuclei, particularly transmuta-

tions, will appear in a later issue of these *Reviews*.

(b) If we take a *simple potential hole* as auxiliary potential, the wave functions are spherical harmonics, multiplied by Bessel functions of order  $l + \frac{1}{2}$  of the radius,  $l$  being the order of the spherical harmonics (azimuthal quantum number). If the walls of the hole are infinitely high, the Bessel functions must vanish for  $r=R$  (nuclear radius). If the height of the walls is finite, this boundary condition has to be relaxed by a more complicated one, involving the wave function and its derivative.

The order of the energy levels has been worked out by Elsasser (E3) for infinitely high walls, by Margenau (M7) for finite walls of a certain height. The arrangement of the energy levels is in both cases similar to that for the oscillator potential, but the "accidental degeneracy" of levels with different  $l$  and the same  $N$  which we found for the oscillator potential, is of course removed. The oscillator level  $N$  splits into levels with given  $l$  and  $n$  in such a way that the level of highest  $l$  lies lowest. The arrangement of the levels is shown in Fig. 8 for the oscillator potential, the potential hole with infinitely high walls, and the potential hole of finite depth, just sufficient to take 58 particles (this is the case considered by Margenau). The figure shows all levels below  $100\hbar^2/MR^2$  in a potential hole of radius  $R$  with infinitely high walls. These levels are also given in Table X. According to our

TABLE X. Energy levels in potential hole with infinite walls. Energy in units  $\hbar^2/MR^2$  where  $R$  = radius of hole.

l	1ST LEVEL OF AZIMUTHAL QUANTUM NUMBER l		2ND		3RD		4TH		l	1ST LEVEL	
	Des.	En.	Des.	En.	Des.	En.	Des.	En.		Des.	En.
0	1s	4.93	2s	19.74	3s	44.42	4s	78.96	6	7i	55.27
1	2p	10.12	3p	29.85	4p	59.45	5p	98.92	7	8j	67.98
2	3d	16.61	4d	41.35	5d	75.96			8	9k	81.79
3	4f	24.40	5f	54.25	6f	93.83			9	10l	96.74
4	5g	33.51	6g	68.49							
5	6h	43.76	7h	83.98							

\* Spectroscopic designation.

\*\* Energy.

scheme, we should expect a successive filling-up of the quantum states with neutrons and protons. The first two neutrons (or protons) will go into the 1s shell, the next six into the 2p shell, etc. The shells are tabulated in Table XI in the order of their energy; below each shell the number of quantum states in it is given ( $n_i$ ); in the third

TABLE XI. Successive filling of neutron (or proton) shells in potential hole with infinitely high walls.

SHELL	1s	2p	3d	2s	4f	3p	5g	4d	6h	3s	5f	7i	4p	8j	6g
$n_i$	2	6	10	2	14	6	18	10	22	2	14	26	6	30	18
$N_i$	2	6	12	14	6	18	34	40	6	48					
$S_i = \sum_{k=1}^i N_k$	2	8	20	34	40	58	92	132	138	186					

line the  $n_i$ 's of shells with nearly identical energy are added ( $N_i$ ); in the last line the  $N_i$ 's of all shells up to the one considered are added: The figures in the last line ( $S_i$ ) therefore represent the numbers of neutrons (or protons) for which we would expect a shell (or group of shells of nearly identical energy) to be completed.

Whenever a shell is completed, we should expect a nucleus of particular stability. When a new shell is begun, the binding energy of the newly added particles should be less than that of the preceding particles which served to complete the preceding shell. We should thus expect that the 3rd, 9th, 21st, etc., neutron or proton is less strongly bound than the 2nd, 8th, 20th.

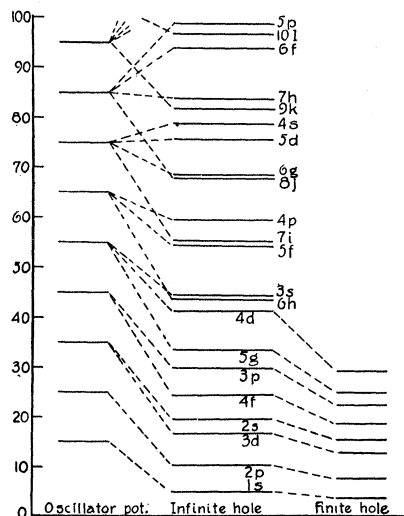
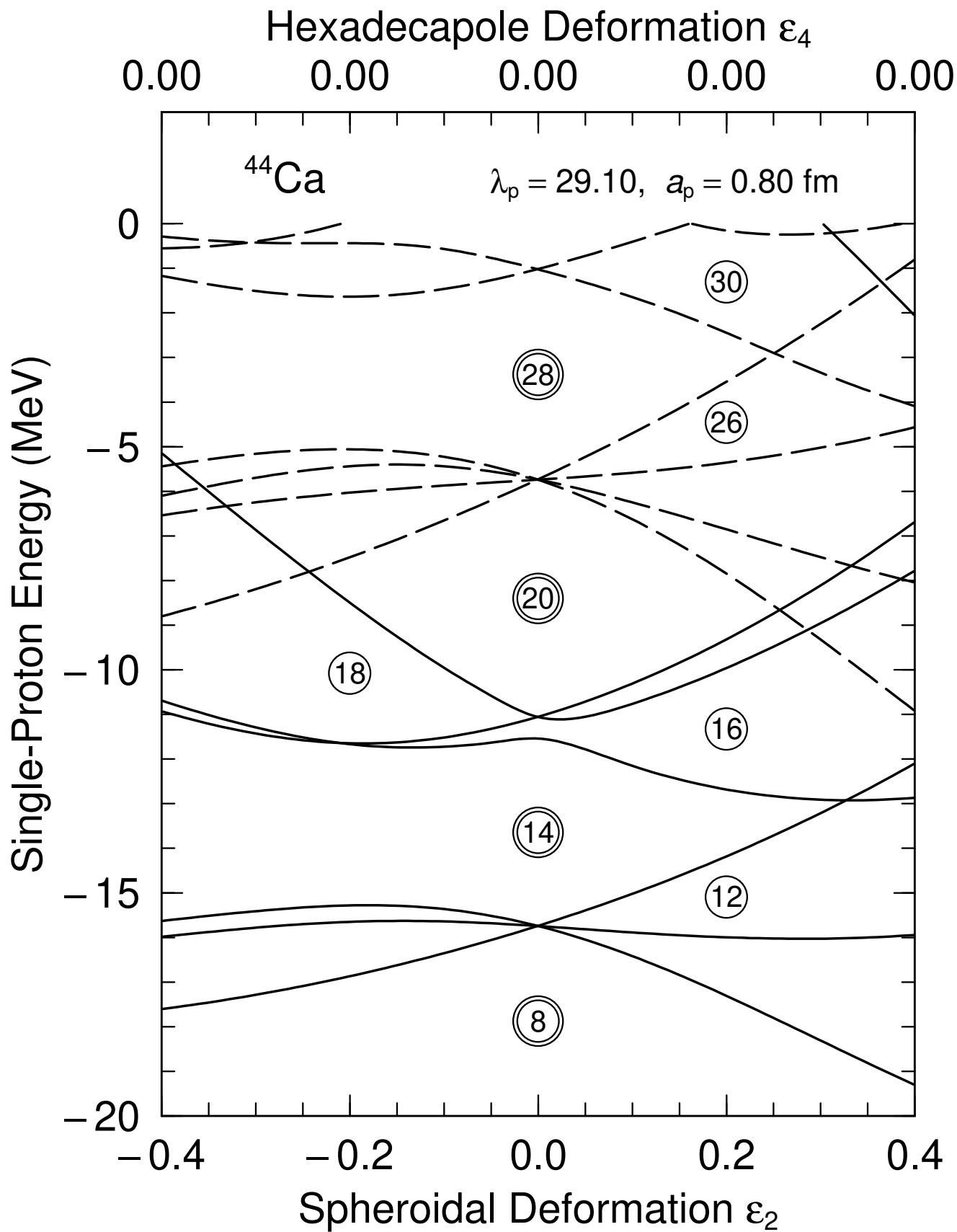
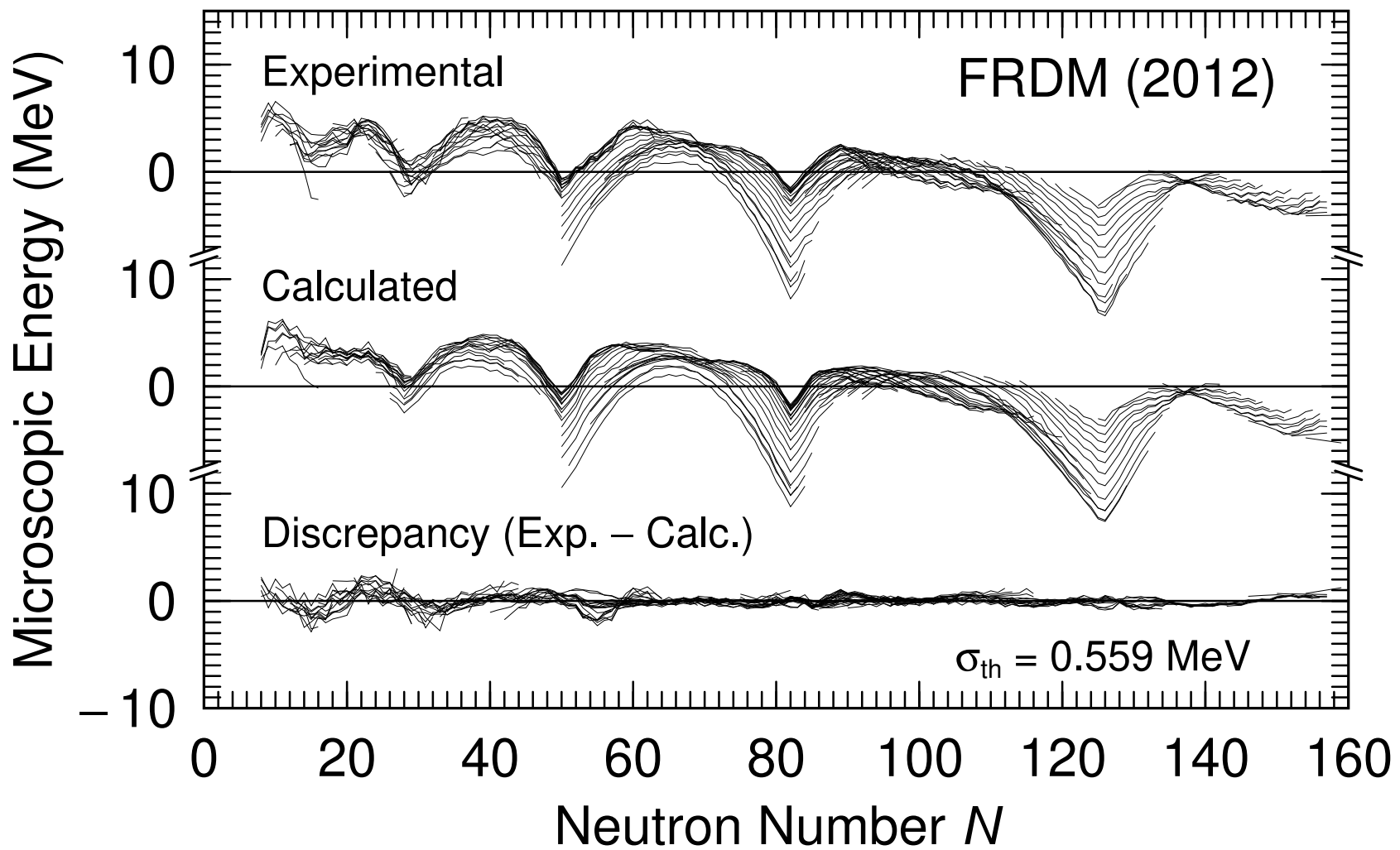


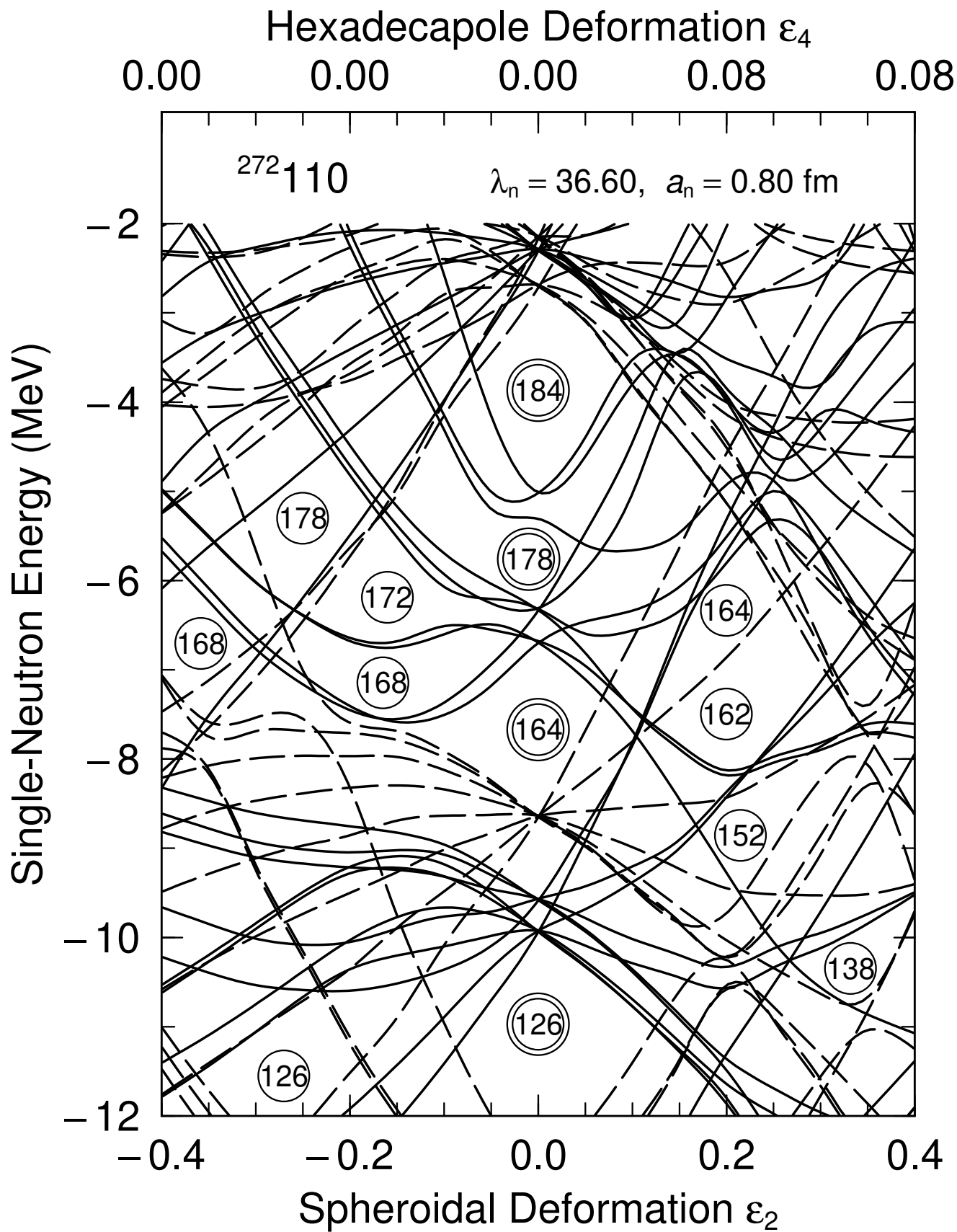
FIG. 8. Energy levels in an oscillator potential, in a potential hole with infinitely high walls, and in a hole with finite walls. The levels in the infinite hole are drawn to scale.

Gaps in single-particle spectra are not always associated with increased stability; it depends on density of levels some distance away. If this density is low e.g. near  $^{40}\text{Ca}$  then no increase in stability, but at  $N = 126$  with high level density above and below then there is a substantial enhancement. For the same reason, for deformed nuclei there is increased stability associated with  $N = 152$  and  $N = 162$ . See next few slides.

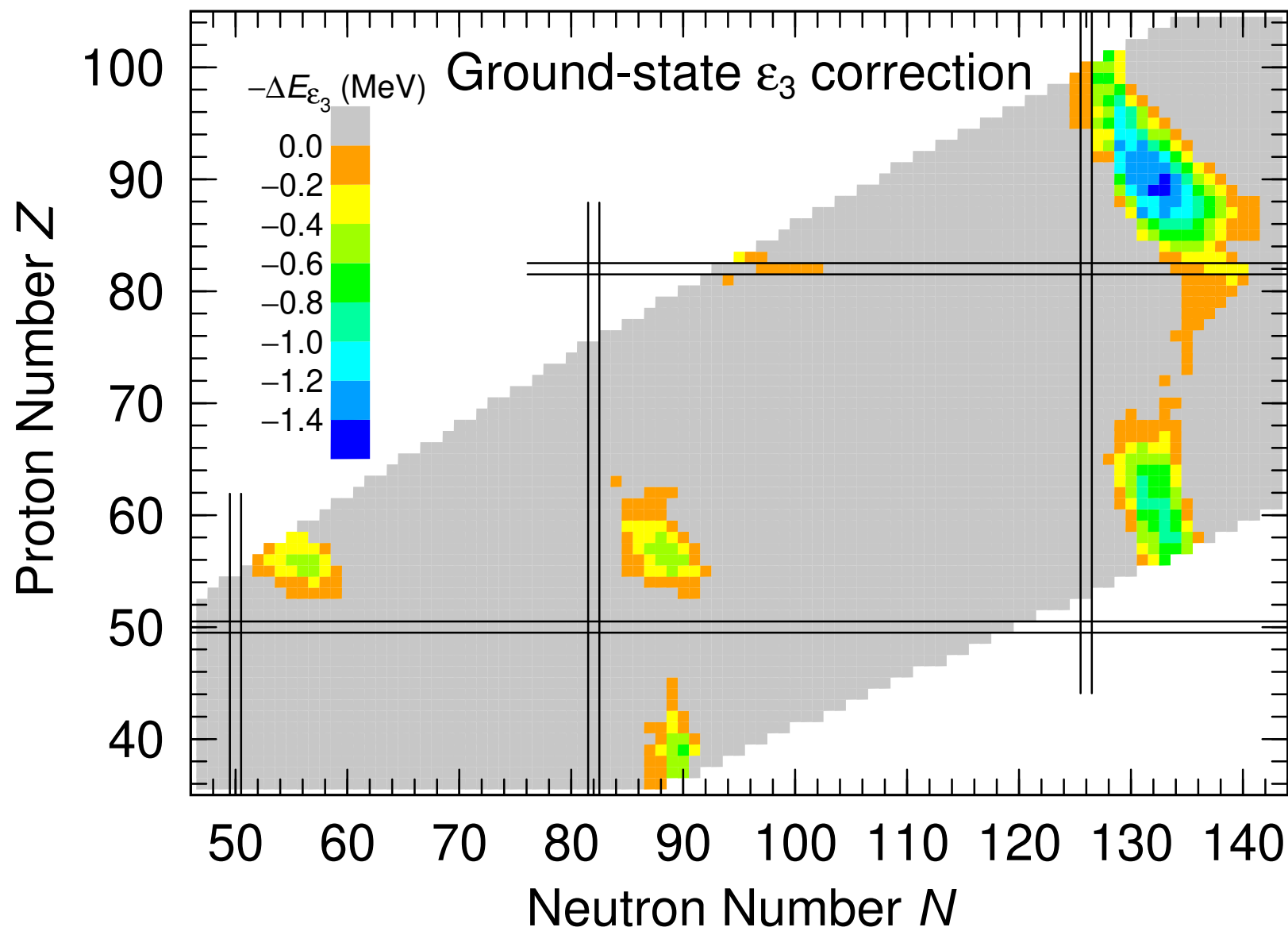


Graph 5

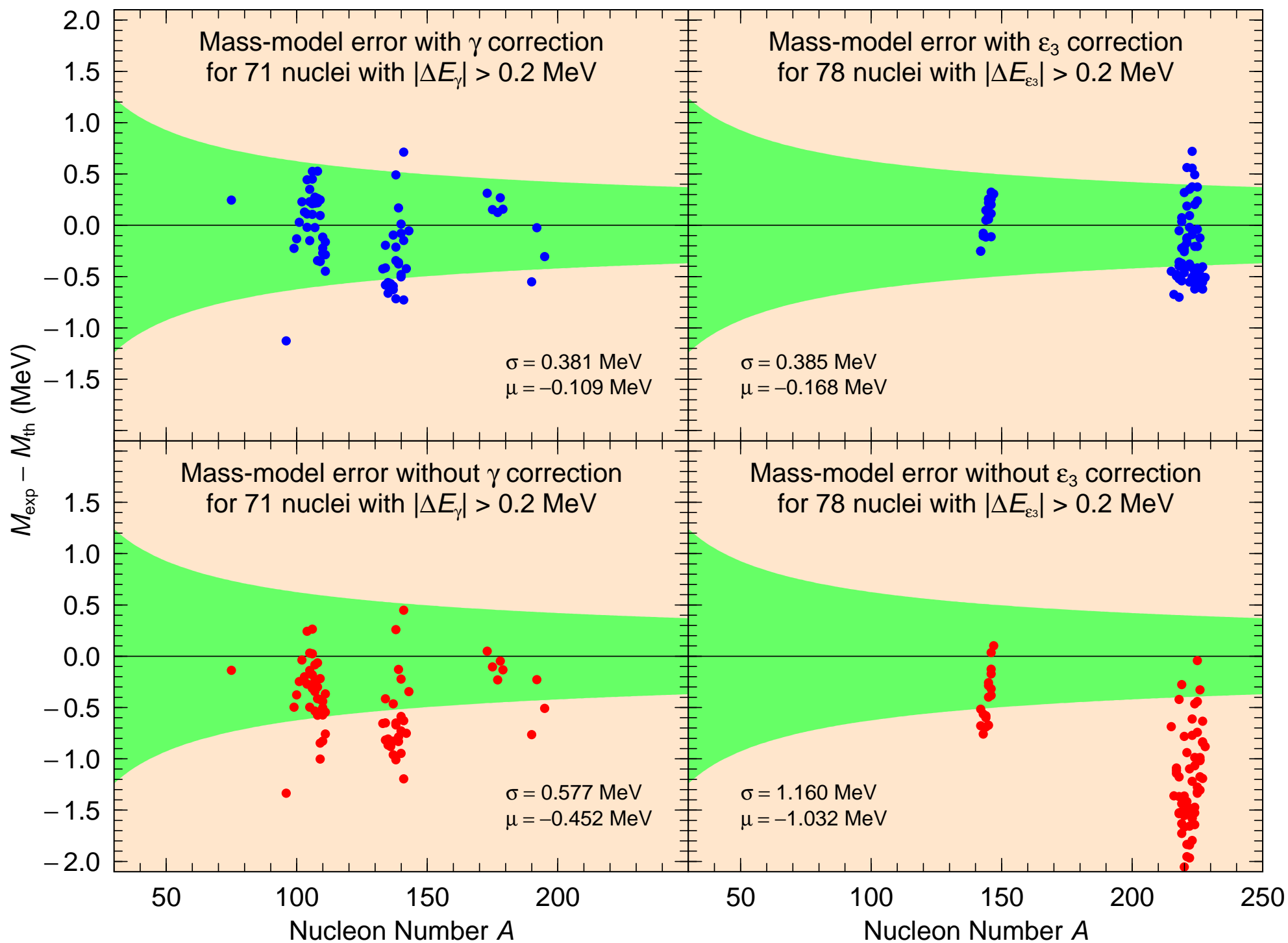




Graph 52



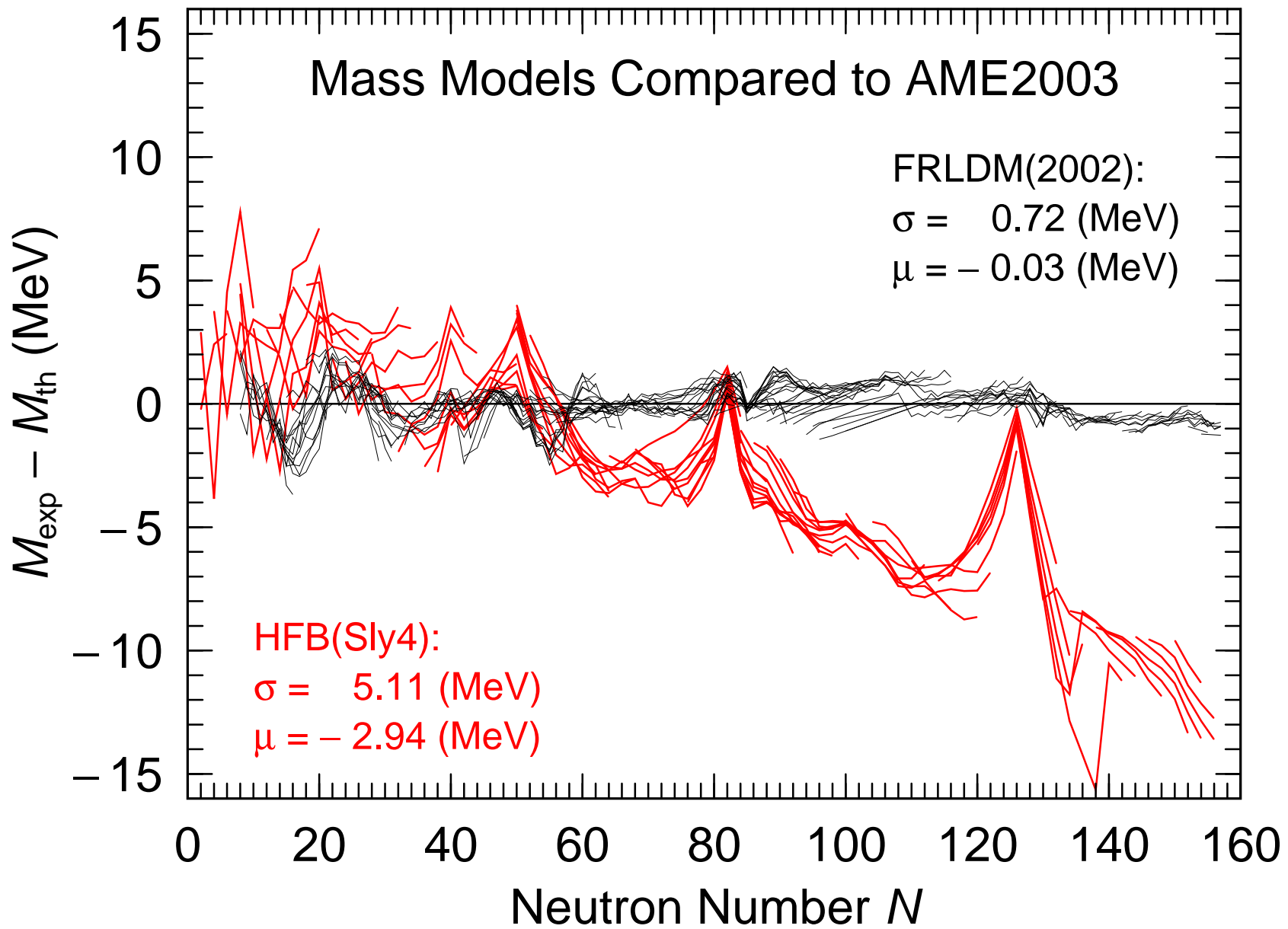
Graph 3





## F E Y N M A N

- Goggle “Feynman I do do not”
- I do not care how clever your model is
- I do not care how smart you are
- If your model does not describe (experimental) data  
IT IS WRONG
- The above he often emphasized in lectures to students
- ME: You actually have to read a paper to have an opinion about it



Since Sly4 (and other) HFB models describe so poorly nuclear ground-state potential energies (masses), in particular near magic numbers, it seems illogical to expect that such potential-energy models are able to describe the fission process. There are also other concerns as discussed earlier.

## S I M P L E      E X P L A N A T I O N

- FEYNMAN: If I cannot explain it simply I have not understood it
- FEYNMAN: How did Schrödinger derive his equation? He did not, it just popped into Schrödinger's head!
- BOHR: If you claim you have “understood” Quantum Mechanics you have not understood it.
- ME: If you think you only need 2D potential-energy plots to understand 5D (or higher) potential-energy results, you have not “understood” it.
- ME (and others) You have found a “simple” explanation if you can use it to predict something “NEW”. Like the asymmetry favoring levels → “rare earth asymmetry”
- ME: So there is no ABSOLUTE requirement that something can be “simply” explained.

## W H A T   I S   A   M O D E L

- Model can be explained
- Results can be reproduced
- Must describe known data
- Must describe new similar data
- Ideally can be generalized to describe new phenomena
- Excellent example: Semi-empirical Mass Model (1936, Bethe-Weizsäcker). Could calculate masses of new isotopes, was subsequently generalized to describe fission.

## TAKE-HOME MESSAGE

- Two INDEPENDENT approaches predict a “rare-earth” (“new”) region of asymmetry.
- One is based on 50+ year old very general model-independent arguments
- The other (BSM) is a QUANTITATIVE method that will give numerical mass-yield curves for any fissioning nucleus at any excitation energy.
- In addition the BSM was benchmarked with respect to the 70 systems studied in 1997 at GSI by KHS and his many collaborators. With very encouraging results.
- So please continue to study the “new” region of asymmetry and, as always, try to falsify the theoretical PREDICTIONS.